Open access • Journal Article • DOI:10.1063/1.370333

Ultrafast ablation with high-pulse-rate lasers. Part I: Theoretical considerations

Eugene G Gamaly, Andrei Rode, Barry Luther-Davies

Published on: 21 Apr 1999 - Journal of Applied Physics (American Institute of Physics)

Topics: Laser ablation, Ultrashort pulse, Laser, Pulsed laser deposition and Nanosecond

JOURNAL OF APPLIED PHYSICS VOLUME 85, NUMBER 8 15 APRIL 1999

Ultrafast ablation with high-pulse-rate lasers. Part I: Theoretical considerations

E. G. Gamaly
Departamento de Fisica, Universidad Autonoma Metropolitana-Iztapalapa, Apartado Postal 55-534, 09340, Mexico D.F., Mexico

A. V. Rode[a] and B. Luther-Davies
Laser Physics Centre, Research School of Physical Science and Engineering, Australian National University, Canberra, ACT 0200, Australia

(Received 4 June 1998; accepted for publication 1 January 1999)

We propose a novel ultrafast pulsed laser deposition (PLD) technique, which eliminates the well-known problem of contamination of the films produced by PLD with particulates ejected from the target. The method uses low energy, picosecond duration laser pulses delivered onto a target at rates of several tens of MHz and thus differs from conventional the PLD method which utilizes high energy, nanosecond duration pulses delivered at low (≈10 Hz) repetition rates. In this article we present the theoretical background justifying the method and define the optimal conditions for efficient evaporation of a target with given thermodynamic properties. By reducing the laser pulse energy while maintaining optimum evaporation, the number of atoms evaporated by each pulse is reduced to the point where it becomes impossible for macroscopic lumps of material to be ejected with the available laser energy, thus preventing the source of particle contamination in the film. To achieve high evaporation rate, the laser pulse repetition rate is increased. We compare our theoretical predictions with literature reports of optimal evaporation in a number of experiments, while in part II of this article we describe a specific experimental study where the method is applied to the production of amorphous carbon thin films. © *1999 American Institute of Physics.* [S0021-8979(99)07307-7]

I. INTRODUCTION

Laser ablation for thin film growth has generated a lot interest in the past few years as one of the simplest and most versatile methods for the deposition of a wide variety of materials. So far most of the work on this so-called pulsed laser deposition (PLD) process has concentrated on the use of high energy excimer or solid-state Nd:YAG lasers whose output is typically 1 J in ≈10 ns duration pulses at a repetition rate of 10–100 Hz.

The major problem with PLD has been the deposition of particulates (or droplets) on the film during the deposition process. The origin of these particles is connected with inhomogeneities in the target, fluctuations in the laser fluence, and other irregularities of the process. The particulate problem severely limits the commercial application of PLD since many of applications of thin film demand the density of micron-sized particles to be less than one per cm^2. While there have been attempts to prevent particles from the target reaching the substrate, using some form of mechanical filtering, there does not appear to have been any satisfactory or universal solution to the problem.

In this article we propose a modification to the PLD process, which we will call ultrafast PLD. Ultrafast PLD employs low energy, picosecond laser pulses at MHz repetition rates for laser ablation and subsequent deposition of thin films. The underlying principles of the method are that individual short low energy pulses will evaporate very few atoms per pulse, thereby inhibiting the ablation of particles or droplets. To compensate for the reduced ablated mass per pulse, high pulse repetition rates are then used to achieve a high averaged deposition rate. The high repetition rate has an additional consequence, namely the pulses are sufficiently closely spaced that the slowest atoms from one pulse arrive at the substrate at the same time as the faster atoms from subsequent pulses. As a result, films grow from a continuous flux of atoms rather than the discontinuous growth characteristic of conventional PLD. Additionally, the use of a high repetition rate laser in turn allows fine control over the deposition process via the repetition rate (e.g., by removal of every nth pulse from the train). To maintain constant ablation rate the ultrafast PLD method requires fast scanning of the laser beam over the target surface. This allows, for example, coevaporation of different materials by scanning across targets of different composition, or rapid successive evaporation of different material. Ultrafast PLD can, therefore, be applied to the production of a range of films from multilayered films, films with mixed composition; and for to the production of monolayers of specific atoms.

The first experiments on the application of ultrafast PLD for deposition of thin carbon films, reported in our earlier conference presentations,[1] demonstrated that extremely high surface quality could be obtained in the deposited carbon films with the total elimination of the particulates from the film. Concurrent with the elimination of particles, an increase in the deposition rate was also achieved, compared to

[a]Electronic mail: avr111@rsphy1.anu.edu.au

the conventional, high power nanosecond PLD.

Thus in summary the key features of ultrafast PLD are: the elimination of particles by reduction of the single pulse energy to the point where fewer atoms are evaporated per pulse than contained in a micron-sized cluster (this corresponds to around 6 orders fewer atoms per pulse than conventional PLD); more efficient evaporation with short picosecond and femtosecond pulses, and the production of a high deposition rate as much as 100 times higher than conventional PLD due to the use of vastly ($>\times 10^7$) higher pulse repetition rates.

In this article we characterize qualitatively and quantitatively the process of vaporization of a target material; the properties of the vapor (plasma) flow; and film deposition on a substrate for high repetition rate laser evaporation. In the first part of the article, we consider target evaporation by a single pulse in different regimes in order to calculate the evaporation rate as a function of absorbed intensity. The relationship between the laser pulse duration, laser flux density, and target parameters for the optimum evaporation is developed as a necessary condition for efficient evaporation. In the second part the average vapor temperature, the required scanning rate, and the evaporation and deposition rates are calculated for the laser-target interaction in a high repetition rate regime. Finally the new vapor–substrate interaction mode which appears when using ultrafast PLD is discussed and compared to the interaction regime encountered in conventional PLD.

II. EVAPORATION OF A SOLID TARGET BY A SINGLE LASER PULSE

A. Laser light absorption

The absorption of laser light in a dielectric at relatively low intensities ($I \leqslant 10^{10}$ W/cm^2) occurs through excitation of the outer atomic electrons. When the excitation energy exceeds the binding energy of the target material, bond breaking may occur and target ablation takes place. For the problem of laser ablation considered in this article, most important are the two limiting cases for deposition of the absorbed laser energy in a target: surface and volume absorption. Surface absorption occurs when the evaporation depth, d, significantly exceeds the absorption length, l_a. Volume absorption takes place when $d \sim l_a$. In both cases the vapor of ablated material must be transparent to the incident radiation.[2–6] Thus, for surface absorption the ablation (absorption) boundary separates the solid and vapour phases of the target material. In this case the evaporation proceeds in the hydrodynamic regime.[2]

At higher intensities, when ionization becomes significant, absorption occurs in the plasma plume at electron densities near the critical density ($n_c \sim \omega^2$ where ω is the frequency of the incident radiation). The main absorption mechanism in this case is inverse Bremsstrahlung.[7] Since the critical density will generally be several orders of magnitude lower than the solid state density of the target, it is not perhaps surprising that a change from surface or volume absorption to absorption in the plasma can markedly affect the laser ablation process. As a result, for any particular target material and laser intensity the absorption mechanism should be specifically identified and the dependence of the flux of ablated vapors on the regime of evaporation and absorption carefully determined.

Below we estimate the flux density of ablated atoms (in [atoms/cm^2 s]) flowing from the target for three different cases of laser absorption: (i) surface absorption when the vapor plume is transparent; (ii) volume absorption in weakly absorbing targets; (iii) absorption at the critical density in an ionized plume.

B. Heat conduction regime

Let us suppose that a laser beam with an energy flux density I_0(W/cm^2) and a pulse duration t_p is incident on a plane solid target. Let us consider various regimes of laser evaporation corresponding to various combinations of pulse duration and laser intensity.

We start with a simple example of a target heated by a single laser pulse in a heat conduction regime where one can neglect losses due to radiation and plume expansion. We assume that the incident laser energy is absorbed in a layer much thinner than the penetration depth of the heat wave. Thus, one can consider the heating process as the propagation of a heat wave into the target in accordance with the one-dimensional heat conduction equation:[8]

$$\frac{\partial T}{\partial t} = a \frac{\partial^2 T}{\partial x^2}, \tag{1}$$

where

$$a = \frac{\kappa}{C_p \rho_0};$$

here a is the thermal diffusion coefficient in [cm^2/s]; κ is the heat conduction coefficient in [J/(s cm K)], C_p is specific heat [J/(g K)], and ρ_0 is target material density in [g/cm^3]. Let us also assume for the sake of simplicity that the laser pulse profile in time has a rectangular shape with a step-like rise and fall: $I = I_a (0 \leqslant t \leqslant t_p)$. Here t_p is the laser pulse duration, and I_a is the absorbed laser intensity. We suppose that the target fills the half space at $x \geqslant 0$, and the energy (heat) flux at the target surface has the same temporal form as the absorbed laser flux. The heat conduction Eq. (1) with these boundary conditions has an exact solution:[8]

$$T(x,t) = \frac{a^{1/2}}{\kappa \pi^{1/2}} \int_0^{t_p} \frac{I_a(\tau)}{(t-\tau)^{1/2}} \exp\left\{ -\frac{x^2}{2a(t-\tau)} \right\} d\tau. \tag{2}$$

It is convenient to introduce the temperature of the heated area of the target averaged over space to the end of laser pulse as follows:

$$\langle T \rangle = \frac{1}{(at_p)^{1/2}} \int_0^{\infty} T(x,t_p) dx. \tag{3}$$

Now one can immediately obtain (for the rectangular shaped pulse) the value of the average temperature as a function of the laser and target parameters in the explicit form:

$$\langle T \rangle = \left(\frac{2}{\pi} \right)^{1/2} \frac{I_a (at_p)^{1/2}}{\kappa} = \frac{1}{2^{1/2}} T(0,t_p). \tag{4}$$

In Eq. (4) we also introduced the average temperature via the surface temperature of the target at the end of the laser pulse, $T(0,t_p)$. One can interpret Eq. (4) as a balance of the absorbed energy flow with heat flux into the target. One should note that the maximum target temperature occurs at the end of the laser pulse, i.e., $T_{\max}=T(0,t_p)$. Therefore, the time dependence of surface temperature during the laser pulse ($t<t_p$) can be written:

$$T(t)=T_m\left(\frac{t}{t_p}\right)^{1/2}. \tag{5}$$

C. The relationship between a laser pulse duration and absorbed intensity for optimum evaporation

Let us assume that the whole thermal energy of the target $E=C_p\rho_0\langle T\rangle$ goes into evaporation. This leads to the highest possible evaporation efficiency and requires the thermal energy to be equal to the heat of evaporation:

$$C_p\rho_0\langle T\rangle=\rho_0\Omega; \tag{6}$$

here $\Omega=\epsilon_b/M[\mathrm{J/g}]$ is the heat of vaporization, ϵ_b is the binding energy, and M is the atomic mass of the target material. Making use of Eqs. (4) and (5) a simple relationship can be obtained between laser and target parameters for optimum evaporation:

$$I_a t_p^{1/2}=\left(\frac{\pi}{2}\right)^{1/2}a^{1/2}\rho_0\Omega. \tag{7}$$

Equation (7) indicates that the product of the absorbed laser intensity and the square root of laser pulse duration should be constant for optimal target evaporation. Thus, changing the pulse duration, for example, from 10 ns to 100 ps the laser intensity should be increased 10 times to maintain optimal evaporation. One also can deduce from Eq. (7) that the evaporation rate in optimum conditions can be written as follows:

$$n_0 v_{\mathrm{evap}}=n_0\left(\frac{a}{t_p}\right)^{1/2}=\left(\frac{2}{\pi}\right)^{1/2}\frac{I_a}{\epsilon_b}. \tag{8}$$

As an example, the relation between laser intensity and pulse duration for optimal evaporation is shown in Fig. 1 for a graphite target with the following parameters:[9] $\kappa=0.063\ \mathrm{W/(cm\,K)}$, $\rho_0=2.26\ \mathrm{g/cm^3}$, $C_p=0.7\ \mathrm{J/(g\,K)}$, $a=4\times10^{-2}\ \mathrm{cm^2/s}$, and $\Omega=3.55\times10^5\ \mathrm{J/mol}$. Also included in Fig. 1, are experimental conditions used for carbon evaporation with various pulse durations from 90 fs to 0.6 ms. The data are a reasonably good fit to Eq. (7), even when the laser pulse duration varies over almost ten orders of magnitude.

D. Target cooling after the end of the laser pulse

Using the exact solutions of the heat conduction equation [Eq. (8)] one can easily find the time dependence of the surface temperature after the end of the laser pulse:

$$T(0,t)=T(0,t_p)\left(\frac{t_p}{t}\right)^{1/2}=\sqrt{\frac{2}{\pi}}\frac{I_a(at_p)^{1/2}}{\kappa}\left(\frac{t_p}{t}\right)^{1/2}. \tag{9}$$

Thus, it follows that for 10 ns laser pulses at a repetition rate of 10 Hz, each pulse arrives when the surface temperature on the target surface has decreased 3×10^3 times (actually, to the room temperature) in comparison with the maximum temperature reached at the end of the previous pulse. For 100 ps pulses at a 100 MHz repetition rate the decrease is only 10 times. The same relation can be applied at the substrate surface to deduce the surface temperature produced by the flux of arriving hot atoms will remain high in the case of high repetition rates but again falls to room temperature between pulses in the case of 10 Hz repetition rates.

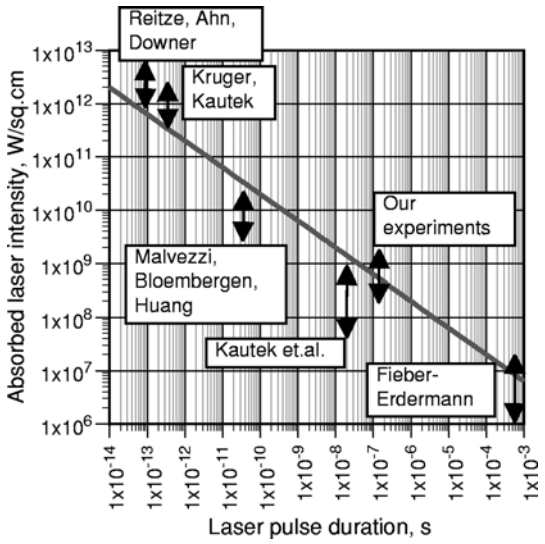

FIG. 1. Absorbed laser intensity as a function of laser pulse duration for optimal evaporation of graphite in accordance with Eq. (7). The arrows show the range of laser intensities in the following experiments (see Refs. 10–15).

E. The evaporation rate

1. The case of absorption at the vapor–solid interface

We assume as before that the evaporation front catches up with the heat front in the early stages of the pulse and later they are moving together. In this case evaporation of the target occurs in a thin layer near the vapor interface where the absorption occurs. We consider the case where the incident intensity is not high enough to produce significant ionization in the plume ($I_a\leqslant10^{10}\ \mathrm{W/cm^2}$) and, therefore, the plume is transparent to the laser beam throughout the interaction time.

This leads to evaporation in an infinitesimally narrow region (surface absorption) and, therefore, all quantities (density, velocity, pressure, and temperature) change in a step-like fashion at the solid–vapor interface. Thus, we arrive at the conventional situation for the interaction between laser radiation and matter where all material parameters at the interface are related to the absorbed laser intensity via conservation laws for mass, momentum, and energy. Let us denote the initial target mass density as ρ_0; and the pressure in a solid as ρ_0; vapor pressure as p_1; vapor velocity as v_1; vapor mass density as ρ_1; and the specific energy of vapor and the velocity of vaporization, correspondingly, as ϵ_1, and v_{evap}. We will further treat the vapor as an ideal gas with an adiabatic exponent γ, and the sound velocity c_1. The impor-

tant characteristic of the target material is the heat of vaporization Ω[J/g], or binding energy per one atom, $\epsilon_b=\Omega\times M$, where M is atomic weight in grams. One can also introduce the characteristic temperature as $T^*=\epsilon_b/k_B$ (k_B is the Boltzmann constant). Thus, one can present the equation of state for the vapor in the form:

$$\epsilon_1=\frac{1}{\gamma-1}\frac{p_1}{\rho_1}+\Omega;$$

$$c_1^2=\gamma\frac{p_1}{\rho_1}=\gamma\frac{k_BT}{M}; \tag{10}$$

$$\rho_1=n_1N; \quad \text{and} \quad p_1=n_1k_BT.$$

The conservation laws on the solid-vapor boundary are as follows:

$$-\rho_0v_{\text{evap}}=\rho_1(v_1-v_{\text{evap}}),$$

$$p_0=p_1-\rho_0v_{\text{evap}}v_1, \tag{11}$$

$$I_a=-\rho_0v_{\text{evap}}\left(\epsilon_1+\frac{v_1^2}{2}\right)+p_1v_1.$$

In general, $v_1\gg v_{\text{evap}}$; therefore we take $v_1\approx c_1$. We can now present Eq. (11) in the following form:

$$P_0=(1+\gamma)n_1k_BT,$$

$$I_a=n_1c_1\left\{\frac{\gamma(1+\gamma)}{2(\gamma-1)}k_BT+\epsilon_b\right\}. \tag{12}$$

Let us introduce the evaporation rate in the form:

$$R_{\text{evap}}=n_1v_1\left[\frac{\text{atoms}}{\text{cm}^2\,\text{s}}\right]. \tag{13}$$

Now making use of Eqs. (10)–(13) we can express the evaporation rate through the absorbed intensity and surface temperature:

$$R_{\text{evap}}=\frac{I_a}{\epsilon_b+k_BT\dfrac{\gamma(\gamma+1)}{2(\gamma-1)}}. \tag{14}$$

For the maximum evaporation rate, and for the maximum deposition rate, the vapor temperature should be low and the following condition should be fulfilled:

$$\epsilon_b\gg k_BT\frac{\gamma(\gamma+1)}{2(\gamma-1)}.$$

In this case, as expected, Eq. (14) gives the same value for the evaporation rate as was obtained in Sec. II C, Eq. (8).

The dependence of vapor density on the temperature cannot be obtained from these relations. To our knowledge, there is no satisfactory analytical relationship between the absorbed laser intensity and the target temperature at low intensities. To obtain a rough estimate one can describe the vapor density in an Arrenius-like form similar to that for saturated vapors:[2–7]

$$n_1=\beta n_0\left(\frac{c_0}{c_1}\right)^3\exp\left\{-\frac{\epsilon_b}{k_BT}\right\}; \tag{15}$$

here c_0 is the speed of sound in a cold target material, and β is numerical constant, which should be determined by experiment.[6] Making use of the previous formula, one easily obtains the relation between the temperature and absorbed laser intensity at the evaporation boundary:[2,3,6]

$$\frac{I_a}{I^*}=\left(\frac{\epsilon_b}{k_BT}+\frac{\gamma(\gamma+1)}{2(\gamma-1)}\right)\exp\left\{-\frac{\epsilon_b}{k_BT}\right\}; \tag{16}$$

where

$$I^*=\frac{\beta}{\gamma}\rho_0c_0^3.$$

For low intensity $\epsilon_b/k_BT\gg 1$ [low vapor temperature limit of the Eq. (14)] and $I_a\gg I^*$ the evaporation rate is expressed as:

$$R_{\text{evap}}\cong\frac{I_a}{\epsilon_b}. \tag{17}$$

For example, from Eq. (17) for optimal laser evaporation of carbon ($\epsilon_b=5.983\times10^{-19}$ J) at an intensity 6×10^8 W/cm^2, the evaporation rate is $\sim10^{27}$ atoms/(cm^2 s). For the high atomic vapor temperature case [upper limit of the Eq. (14)] the evaporation rate can be written as follows:

$$R_{\text{evap}}\cong\frac{I_a}{k_BT\cdot\dfrac{\gamma(\gamma+1)}{2(\gamma-1)}}. \tag{18}$$

It appears that for highly refractory materials, such as carbon, the condition that the plume must be transparent fails at a high temperature. Later we will use the low temperature formula as the refractory materials are of a major concern in this article.

Now one can compare the evaporation rates when using 10 ns and 100 ps laser pulses for optimum evaporation regime in accordance with Eq. (7). It is easy to observe from Eqs. (7) and (17) that for optimum evaporation regime and for laser interaction with a transparent plume, the evaporation rate is expressed as:

$$nv\sim I_a\sim t_p^{-1/2}. \tag{19}$$

Therefore, the transition from a long 10 ns pulse to a short 100 ps pulse results in ten fold increase of the evaporation rate (in [cm^{-2} s^{-1}]) per single pulse. As an example, the increase in the evaporation rate with the decrease in the laser pulse duration at optimal laser intensity for a graphite target is shown in Fig. 2. For comparison, we derived the evaporation rate from the volume of the crater reported in several experiments.[10,11,13,14] The experimental data shows a good fit to Eq. (14).

Other important characteristics of the single pulse interaction are the evaporation velocity and the evaporation (etched) depth d, which can be easily recovered from the previous formula as:

$$v_{\text{evap}}=\frac{I_a}{n_0\cdot\epsilon_b}; \tag{20}$$

and

$$d=v_{\text{evap}}\cdot\tau_{\text{las}}. \tag{21}$$

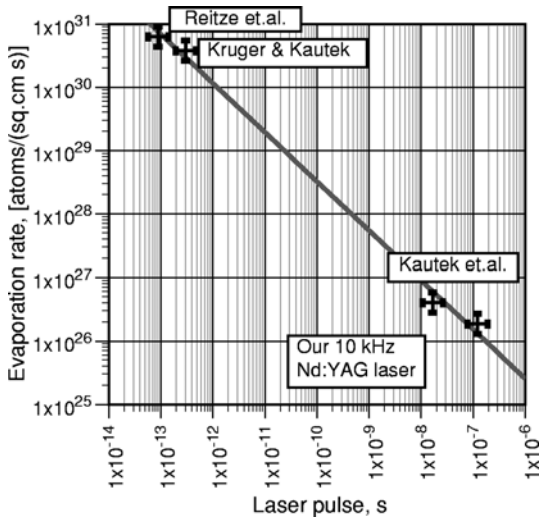

FIG. 2. Evaporation rate of the graphite target for the optimal evaporation with different laser pulse durations in accordance with Eq. (14). The crosses are results derived from the following experiments (see Refs. 10, 11, 13, and 14).

For example, in the case of optimal evaporation of a graphite target ($n_0 = 10^{23}\,\mathrm{cm}^{-3}$, $\epsilon_b = 5.983\times10^{-19}\,\mathrm{J}$) by a 60 ps laser pulse at the average intensity of $\sim 10^{10}\,\mathrm{W/cm^2}$ the evaporation depth per pulse equals $d \sim 1000\,\text{Å}$.

It is worth noting here that the laser absorption, and consequently the evaporation rate, depend on laser intensity [$\mathrm{W/cm^2}$], not on laser fluence [$\mathrm{J/cm^2}$] as has been suggested in some articles on laser deposition. However, as one can see from the Eqs. (20) and (21), the etched depth is determined by the laser fluence.

2. The case of volume (low) absorption

Let us consider the case when the evaporation depth is close to the absorption depth ($d \approx l_a$) and absorption occurs in volume of heated material. In accordance with Refs. 2 and 6, the characteristic density of the ablated material remains constant during the evaporation and ablation process. Therefore, to describe the process one needs only the two conservation laws for momentum and energy. For this case the general formula for evaporation rate in Eq. (14) remains valid. The essential difference between volume (weak) absorption and surface (strong) absorption relates to the fact that in a volume absorption the heat of evaporation depends on the temperature of the medium and goes to zero when the temperature reaches the critical temperature.[8] Thus, we can easily represent the maximum evaporation rate for volume absorption in the form:

$$R_{\mathrm{evap}} \cong \frac{I_a}{k_B T_{\mathrm{cr}} \dfrac{\gamma(\gamma+1)}{2(\gamma-1)}}, \tag{22}$$

where T_{cr} is the critical temperature for the target material. For a carbon target, taking $T_{\mathrm{cr}} \sim 4.5\times10^3\,\mathrm{K}$ and $\gamma = 5/3$, we find that the maximum evaporation rate from Eq. (22) is 2.86 times higher than in the case of Eq. (17).

3. The case of absorption in a plasma layer

Let us consider, for comparison, the case of absorption in a plasma when the laser light is absorbed near the critical electron density.[7,16] This becomes important at a relatively high intensity ($>10^{10}$–$10^{11}\,\mathrm{W/cm^2}$) where ionization of the plume takes place and the Inverse Bremsstrahlung mechanism of absorption plays a major role. The characteristic density of vapors is the critical density n_c:[7]

$$n_e = Z n_i \cong n_c = \frac{m_e \omega_l^2}{4\pi e^2} = 1.16\times10^{21}\left(\frac{1\,\mu\mathrm{m}}{\lambda}\right)^2; \tag{23}$$

here m_e, ω_l, λ, and e, respectively, are electron mass, laser frequency, laser wavelength (in [μm]), and electron charge. The evaporation rate can be expressed as above, through the absorbed laser intensity and surface temperature, taking into account the ionization losses per atom ϵ_{ion}:

$$R_{\mathrm{evap}} = n_1 v_{\mathrm{evap}} = n_c\left(\frac{\gamma k_B T}{M}\right)^{1/2} = \frac{I_a}{\epsilon_b + \epsilon_{\mathrm{ion}} + k_B T \dfrac{\gamma(\gamma+1)}{2(\gamma-1)}}; \tag{24}$$

here $\epsilon_{\mathrm{ion}} = \Sigma_i \alpha_i^{\mathrm{ion}} J_i$, the summation extends over all ionization stages, α^{ion} is the ionization rate, and J_i is the ith ionization potential. In the absence of ionization, the Eq. (24) transforms into Eq. (14) for atomic vapor. The surface temperature can be calculated as a function of the absorbed laser intensity and laser wavelength:

$$\left(\frac{k_B T}{\epsilon_b + \epsilon_{\mathrm{ion}}}\right)^{1/2}\left[1 + \frac{k_B T}{(\epsilon_b + \epsilon_{\mathrm{ion}})}\,\frac{\gamma(\gamma+1)}{2(\gamma-1)}\right] = \frac{I_a}{I^{**}}, \tag{25}$$

where I^{**} is the characteristic intensity

$$I^{**} = n_c \gamma^{1/2} \frac{(\epsilon_b + \epsilon_{\mathrm{ion}})^{3/2}}{M^{1/2}}, \tag{26}$$

which is in inverse proportion to the square of the laser wavelength. For example, for carbon target at $I_a = 10^9\,\mathrm{W/cm^2}$, one obtains $k_B T = 2$ eV from Eq. (25).

Next we estimate the absorption coefficient in the critical density region. The Inverse Bremsstrahlung absorption (collisional absorption) mechanism has been studied thoroughly both theoretically and experimentally over several decades. To estimate the absorption coefficient A one can use a well-established approximation for a plasma with a linear density gradient ($n_e = n_c(x/L)$ (Ref. 7):

$$A = 1 - \exp\left\{-\frac{8\nu_c L}{3c}\right\}; \tag{27}$$

here c is the speed of light in vacuum, ν_c is a collision rate at $n_e = n_c$, and L is the characteristic length scale of the expanding plasma density profile ($L = v_{\mathrm{evap}} \cdot t_p$). The collision rate can be written:[7]

$$\nu_c = 3.342\,\frac{e^4}{m_e^{1/2}}\,\frac{n_c Z \ln\Lambda(n,T_e)}{T_e^{3/2}} \cong 3\times10^{-6}\,\frac{n_c Z \ln\Lambda(n,T_e)}{T_e^{3/2}}, \tag{28}$$

where $\ln\Lambda(n,T_e)$ is the Coulomb logarithm[7] and T_e is in eV. Taking $Z = 1$, $I_a = 10^9\,\mathrm{W/cm^2}$, $v_{\mathrm{evap}} = 4\times10^5\,\mathrm{cm/s}$, $T_e = 2$ eV, $n_c = 10^{21}\,\mathrm{cm}^{-3}$, and $\ln\Lambda = 3.78$, the electron-ion col-

lision frequency from Eq. 28 is $\nu_c \approx 4.6\times 10^{15}\,\mathrm{s}^{-1}$. Assuming that for 120 ns laser pulse $L=4.8\times 10^{-2}$ cm, Eq. (28) gives the absorption $A\approx 1$. This value corresponds well with the measured absorption in a graphite target ~85%.[14]

III. TARGET HEATING BY A TRAIN OF LASER PULSES (REPETITIVE PULSE REGIME)

When searching for the optimum evaporation regime, one should consider two broad and overlapping constraints. First, it is necessary to achieve efficient evaporation and obtain a high flux of evaporated atoms at an appropriate temperature; second, it is necessary to find the appropriate conditions of the vapor–substrate interaction in order to create precisely the desired structure of the film deposited on the substrate. It seems obvious that in order to keep the laser–target interaction process in the chosen regime, it is necessary to scan the laser beam over the target surface. The minimum scanning velocity can be estimated as follows.

A. Scanning speed

If the focal spot of the laser beam remains on the same spot on the target for many consecutive pulses, a crater will be cut into the target increasing by a depth d each pulse. This crater will confine the vapor plum and increase its density. As a result the light will be absorbed in the vapor and consequently, the interaction regime becomes less favorable for efficient evaporation. When the crater depth is comparable with the diameter of the focal spot, expansion of the vapor plume will be completely different from that from a flat target. In a deep crater the thermal losses into the walls of the crater dominate the laser–target interaction process. Thus, the interaction would change from the optimum case when $d_{\mathrm{hole}} \sim d_{\mathrm{foc}}$.

We present in part II of this article[14] experimental studies on the evaporation of a target by an ultrahigh repetition rate (7.6×10^7 pulses/s, 60 ps) laser focused to a 15 μm spot. According to the estimates above [Eqs. (20) and (21)], the laser increases the depth of the crater by ~100 Å for each pulse. Therefore, to evaporate a hole as deep as the focal spot diameter, one needs $d_{\mathrm{foc}}/d = 15[\mu\mathrm{m}]/100[\text{Å/pulse}] = 1.5\times 10^3$ pulses, or in 2×10^{-5} s. The scanning velocity of the focal spot on the target surface should be higher than $15[\mu\mathrm{m}]/2\times 10^{-5}[\mathrm{s}] = 75$ cm/s.

B. Evaporation rate

We now estimate the net evaporation rate for lasers with a different pulse duration and repetition rates, R_{rep}. The number of atoms evaporated per single pulse can be expressed as:

$$N_{\mathrm{pulse}} = R_{\mathrm{evap}} S_{\mathrm{foc}} \tau_{\mathrm{las}}. \tag{29}$$

The deposition rate is proportional to the number of atoms evaporated per second

$$N\left[\frac{\mathrm{atoms}}{\mathrm{s}}\right] = N_{\mathrm{pulse}} R_{\mathrm{rep}} = R_{\mathrm{rep}} R_{\mathrm{evap}} S_{\mathrm{foc}} \tau_{\mathrm{las}}. \tag{30}$$

Following from the previous sections, $R_{\mathrm{evap}} \sim nv \sim (I_a)^q$ where $q=(1/3 \text{ or } 1)$, depending on the particular regime of the laser–target interaction. For optimum evaporation, one should keep the product $I_a \cdot (t_p)^{1/2}$ constant. Thus, the number of particles evaporated per second in the repetitive pulse regime can be expressed as:

$$N \sim t_p^{1-(q/2)} S_{\mathrm{foc}} R_{\mathrm{rep}}. \tag{31}$$

A comparison of a 10 ns, 30 Hz laser evaporation at $S_{\mathrm{foc}} \sim 0.06\,\mathrm{cm}^2$, to a 60 ps, 76 MHz laser evaporation at $S_{\mathrm{foc}} \sim 10^{-6}\,\mathrm{cm}^2$ gives for $q=1$:

$$\frac{N_{\mathrm{pico,MHz}}}{N_{\mathrm{nano,Hz}}} \cong 3. \tag{32}$$

As a consequence, one finds that the net time averaged ablation rate for the mode-locked laser is similar to that for the low repetition rate Q-switched system of the same average laser power.

C. Deposition rate

If the distance between the target and the substrate is R_0, then the deposition rate N_{dep} and the deposited film thickness d_{dep} per second, by definition, are:

$$N_{\mathrm{dep}} = \frac{N}{2\pi R_0^2}\left[\frac{\mathrm{atoms}}{\mathrm{cm}^2\,\mathrm{s}}\right] \tag{33}$$

and

$$d_{\mathrm{dep}} = \frac{N_{\mathrm{dep}}}{n_{\mathrm{dep}}}\left[\frac{\mathrm{cm}}{\mathrm{s}}\right], \tag{34}$$

here n_{dep} is the number density of the deposited film. Let us take an evaporation rate $R_{\mathrm{evap}} \sim 3\times 10^{28}\,\mathrm{cm}^{-2}\,\mathrm{s}^{-1}$, $S_{\mathrm{foc}} = 10^{-6}\,\mathrm{cm}^2$, $t_p = 6\times 10^{-11}$ s, and a 76 MHz repetition rate. That gives $N_{\mathrm{pico,MHz}} \sim 1.4\times 10^{20}\,\mathrm{s}^{-1}$. Assuming that the density of the deposited carbon film is the same as the carbon target, and the angular distribution of evaporated atoms is homogeneous over a hemisphere with $R_0 = 15$ cm, one readily obtains the estimate for the deposition rate for a 76 MHz laser of $d_{\mathrm{dep}} \approx 80$ Å/s. For a typical target-substrate distance $R_0 = 2$ cm in many laser deposition experiments the deposition rate for 76 MHz laser would be up to 4.5×10^3 Å/s. We should note here that the estimates are for the optimal regime of evaporation at a laser intensity of $2\times 10^{10}\,\mathrm{W/cm}^2$ for a 60 ps pulse.

D. Surface temperature of the target in the case of a succession of laser pulses

With high repetition rate lasers the laser–target interaction occurs in the single pulse regime if the focused laser beam is scanned sufficiently fast over the target surface. However, at the MHz-range laser repetition rate this is not always the case. The process of heating the target surface by a single laser pulse, and the cooling of the surface afterwards, considered in the heat conduction interaction mode of Secs. II C and II D, may be easily generalized to the case where the target surface is heated by succession of laser pulses.

Let us consider now the target surface temperature after it was heated by a succession of n laser pulses of pulse duration t_p following with time intervals t_{pp} ($t_{\mathrm{pp}} \approx 1/R_{\mathrm{evap}}$ for

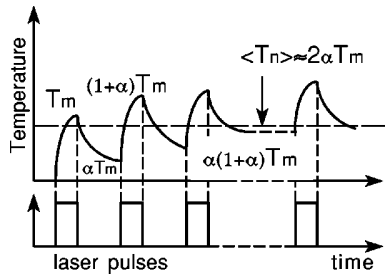

FIG. 3. Temperature of the target surface heated by a series of laser pulses.

$t_p \ll t_{pp}$). The maximum target surface temperature at the end of a single laser pulse is T_{max} and the temperature at the beginning of the following laser pulse is $T_{min} = T_{max}(t_p/t_{pp})^{1/2}$. The ratio for the previous maximum and the following minimum for all laser pulses with the fixed repetition rate is constant and equal to $\alpha = (t_p/t_{pp})^{1/2}$. Now one can easily calculate the maximum and minimum temperatures of the target surface after the action of any number of pulses. Due to the linear character of the heating process the maximum and minimum temperatures from the heating of a succession of n laser pulses are (Fig. 3):

First pulse: $(T_{max})_1 = T_m$; $(T_{min})_1 = \alpha T_m$;

Second pulse: $(T_{max})_2 = (1+\alpha)T_m$;

$$(T_{min})_2 = \alpha(1+\alpha)T_m; \tag{35}$$

nth pulse: $(T_{max})_n = (1+\alpha+\alpha^2+\alpha^3+\cdots+\alpha^{n-1})T_m$

$$= [(1-\alpha^n)/(1-\alpha)]T_m$$

$$\approx (1-\alpha)^{-1}T_m;$$

and $(T_{min})_n = \alpha(T_{max})_n$.

The surface temperature averaged by time over the interaction time is expressed as:

$$\overline{T} = \frac{1}{t}\int T(0,t)dt. \tag{36}$$

Let us denote the target surface temperature defined by Eqs. (4) and (9) after the ith pulse ($t > t_p$) as:

$$T_i(0,t) = T_{m,i}\left(\frac{t_p}{t}\right)^{1/2}. \tag{37}$$

Inserting Eqs. (37) and (5) into Eq. (36) one obtains the surface temperature averaged over any ith laser pulse and the time gap between ith and $(i+1)$th pulses:

$$\overline{T_i} = \frac{1}{t_p+t_{pp}}\int_0^{t_p+t_{pp}} T_{m,i}(0,t)dt = 2\alpha T_{m,i}\frac{(1-\frac{2}{3}\alpha)}{(1+\alpha^2)}. \tag{38}$$

Let us now average the temperature over the all n pulses:

$$\overline{T_n} = \frac{1}{n}\sum_{i=1}^{n}\overline{T_i}.$$

Making use of Eq. (38) one can obtain the average surface temperature after n pulses:

$$\overline{T_n} = \frac{1}{n(t_p+t_{pp})}\int_0^{n(t_p+t_{pp})} T(0,t)dt$$

$$= 2\alpha\frac{\left(1-\frac{2}{3}\alpha\right)}{(1+\alpha^2)}\cdot\frac{1}{n}\sum_{i=1}^{n}\overline{T}_{max,i}, \tag{39}$$

where

$$\sum_{i=1}^{n}\overline{T}_{max,i} = T_m\left(1+\frac{1-\alpha^2}{1-\alpha}+\cdots+\frac{1-\alpha^n}{1-\alpha}\right)$$

$$= \frac{T_m}{(1-\alpha)}\left(n+\frac{\alpha^n-\alpha}{1-\alpha}\right).$$

Now the average temperature can be presented in the final form:

$$\overline{T_n} = 2\alpha\frac{(1-\frac{2}{3}\alpha)}{(1+\alpha^2)}\cdot\frac{T_m}{(1-\alpha)}\left(1+\frac{\alpha^n-\alpha}{n(1-\alpha)}\right). \tag{40}$$

In the case $n \gg 1$ and $\alpha \ll 1$ (Fig. 3):

$$\overline{T_n} \cong 2\alpha T_m = 2T_m\left(\frac{t_p}{t_{pp}}\right)^{1/2}.$$

As one can see, the average target surface temperature is proportional to the maximum surface temperature T_m reached at the end of the laser pulse in a single-pulse regime, and to a square root of the product of the pulse duration and the laser repetition rate.

Applying the same heating-cooling approach to the substrate heated by the flow of hot atoms from the target, one can estimate the average substrate temperature. It is obvious that the increase in laser repetition rate decreases the time interval between the arriving atoms and hence results in increase of the substrate temperature. We will consider the kinetic processes of vapor propagation and the energy transfer from the atom flow to the substrate elsewhere.

E. Comparison of different heating regimes

In order to understand the differences between a heating regimes with the different pulse duration and repetition rate let us compare the average target temperatures for three lasers with the same average power P (typically, it is about 25 W):

(1) conventional low repetition rate high power laser: $R_{rep} = 30$ Hz, pulse duration $t_p = 10$ ns, $\alpha = (t_p R_{rep})^{1/2} = 5.5 \times 10^{-4}$. Let us consider the optimal evaporation regime according to Eq. (7). Note, that $T_{max} \sim I_a(t_p)^{1/2}$; thus $\overline{T_n} \sim 2\alpha T_{max} \sim 10^{-3}\cdot T_{max}$;

(2) high repetition rate laser: $R_{rep} = 10$ kHz, pulse $t_p = 120$ ns; $\alpha = (t_p R_{rep})^{1/2} = 3.5\times 10^{-2}$; $\overline{T_n} \sim 2\alpha T_{max} \sim 0.07\cdot T_{max}$;

(3) ultrahigh repetition rate laser: $R_{rep} = 76$ MHz, short pulse $t_p = 60$ ps, $\alpha = (t_p R_{rep})^{1/2} = 6.75\times 10^{-2}$; $\overline{T_n} \sim 2\alpha T_{max} \sim 0.135\cdot T_{max}$.

Comparing the average target surface temperature for various pulse regimes we can conclude that: (i) for conventional

30 Hz laser evaporation the target completely cools between the pulses; and (ii) increasing the repetition rate increases the temperature to levels much higher than that available with existing continuous wave (cw) lasers. Achieving the optimal evaporation temperature (and consequently a high substrate temperature) with cw laser would require an average laser power above 10 kW. Thus, this comparison demonstrates the advantage of using a high repetition rate, short pulse laser for achieving almost continuous vapor flow from a graphite target, and continuous interaction of carbon vapor with the substrate.

F. The mode of vapor–substrate and vapor–vapor interaction for ultrafast laser ablation and deposition

The vapor–substrate and vapor–vapor interaction starts when the evaporated atoms arrive from the target, hit the substrate surface, and bounce from the surface. There are three kinds of collisions that may occur at that stage: elastic collision when atoms bounce back, nonelastic collisions producing excitations, and sticky collisions leading to atom-to-atom attachment, i.e., structure formation. The vapor–vapor collision time depends on the carbon density near the substrate surface and the vapor temperature. For continuous structure growth the collision frequency and the energy of the interacting atoms should be constant.

At the ultrahigh repetition rate ($\sim$100 MHz) regime of evaporation the time duration between pulses is $\sim 10^{-8}$ s. As follows from the previous analysis the temperature at the evaporation surface is around 10^4 K which implies the average velocity of carbon atoms in the vapours flow is $\nu_s = 4 \times 10^5$ cm/s, and velocity of an expansion front is approximately $\sim 3\nu_s \approx 10^6$ cm/s. Now one can see the difference between the interaction regimes for a nanosecond-range 10 Hz laser, and a picosecond multi-MHz laser. In high repetition rate case the fast atoms evaporated later in time overtake the slow atoms from the earlier evaporated group of atoms. As a result, the space distribution of atoms from the consecutive laser pulses overlaps to form a continuous flow of atoms with chemically active bonds, which is the most appropriate for structure formation. This continuous flow of atoms along with the almost constant collision frequency allows for the formation of elongated structures on the substrate surface. The number of atoms hitting the substrate per second (vapor–substrate collision rate) is $\sim 10^{12}\,\mathrm{s}^{-1}$ while vapor–vapor collision rate is $(\sigma \cdot n\nu) = (10^{-15}\,\mathrm{cm}^2 \times 10^{14}\,\mathrm{cm}^{-3} \times 2 \times 10^5\,\mathrm{cm/s}) \sim 2 \times 10^4\,\mathrm{s}^{-1}$. Therefore, the vapor–substrate collisions play a dominant role in the film formation. We expect that in the ultrafast evaporation regime crystalline elongated structures could be formed on a substrate surface. We would like to stress the importance of kinetic effects in the formation process. By varying the ambient gas and its temperature one can impose greater control on creation of different structures. We will consider this problem in detail elsewhere.

IV. CONCLUSIONS

We have presented, to our knowledge, the first theoretical investigation of laser–target interaction for the ultrafast laser evaporation with multi-MHz repetition rate lasers.

Ultrafast laser ablation with high repetition rate, picosecond pulsed lasers leads to a number of new opportunities for laser deposition technology. First, due to the low number of atoms evaporated per laser pulse the problem of cluster or droplet contamination of the laser plume can be completely resolved. This removes the major disadvantage of laser ablation with conventional low repetition rate powerful lasers, which is the formation of particulates on the substrate surface. Second, we demonstrated that the transition from a nanosecond pulse duration to a picosecond pulse duration leads to a significant increase in the evaporation rate, provided the laser intensity is optimal for the particular target material. Third, high repetition rate leads to a continuous flow of evaporated atoms in the laser plume and thus to an increase in the average surface temperature of a substrate. This could lead to the formation of crystalline structures on the substrate surface, making it possible to control the structure formation through the appropriate choice of the laser parameters in correspondence with the properties of the target.

ACKNOWLEDGMENT

A.V.R. gratefully acknowledges the support of the ARC QE-II Fellowship.

[1] A. V. Rode, E. G. Gamaly, and B. Luther-Davies, in *XX International Quantum Electronics Conference, Sydney, Australia, 14–19 July 1996* OSA Technical Digest Series (Optical Society of America, Washington D.C., 1996), p. 137; A. V. Rode, E. G. Gamaly, and B. Luther-Davies, in XI Australian Optical Society Conference Book of Abstracts, Adelaide, Australia, 10–12 December 1997 (unpublished), p. W4; E. G. Gamaly and A. V. Rode in *High-Power Laser Ablation*, edited by C. R. Phipps, Proc. SPIE **3343**, 847 (1998); A. V. Rode, Luther-Davies, and E. G. Gamaly, in *High-Power Laser Ablation*, edited by C. R. Phipps, Proc. SPIE **3343**, 903 (1998).

[2] Yu. V. Afanasiev and O. N. Krokhin, in *Physics of High Energy Density* (Proceedings of the International School of Physics ''Enrico Fermi'') Course XLVIII, edited by P. Calderola and H. Knoepfel (Academic, New York, 1971).

[3] Yu. V. Afanasiev and O. N. Krokhin, in *Quantum Electronics in Lasers and Masers*, edited by D. V. Skobel'tsyn, Proceedings of the P. N. Lebedev Physical Institute (Consultants Bureau, New York, 1972), Vol. 52, pp. 109–157.

[4] I. Anisimov, Ya. A. Imas, G. S. Romanov, and Yu. V. Khodiko, *The Effect of High Power Radiation on Metals* (in Russian) (Nauka, Moscow, 1970).

[5] A. Vedenov and G. G. Gladysh, *The Physical Processes During the Laser Treatment of Metals* (in Russian) (Energoizdat, Moscow, 1985).

[6] Yu. V. Afanasiev, V. A. Isakov, I. N. Zavestovskaya, B. N. Chichkov, F. von Alvensleben, and H. Welling, Appl. Phys. A: Solids Surf. **64**, 561 (1997).

[7] W. L. Kruer, *The Physics of Laser Plasma Interaction* (Addison–Wesley, New York, 1987).

[8] L. D. Landau and E. M. Lifshitz, *Fluid Mechanics (Course of Theoretical Physics, v. 6)* (Pergamon, Oxford, 1987).

[9] O. Pierson, *Handbook of Carbon, Graphite, Diamond and Fullerenes* (Noyes, Park Ridge, 1993).

[10] D. H. Reitze, H. Ahn, and M. C. Downer, Phys. Rev. B **45**, 2677–93 (1992).
[11] J. Krüger and W. Kautek, Appl. Surf. Sci. **106**, 383 (1996).
[12] A. M. Malvezzi, N. Bloembergen, and C. Y. Huang, Phys. Rev. Lett. **57**, 146 (1986).
[13] W. Kautek, S. Pentzien, A. Conradi, J. Krüger, and K.-W. Brzezinka, Appl. Surf. Sci. **106**, 158 (1996).
[14] A. V. Rode, B. Luther-Davies, and E. G. Gamaly, J. Appl. Phys. **85**, 4222 (1998).
[15] M. Fieber-Erdmann, R. Stübner, A. Ding, T. Beck, and H.-G. Eberle, in *Electronic Properties of Novel Materials: Progress in Fullerene Research* (World Scientific, Singapure, 1994), pp. 62–65.
[16] Yu. V. Afanasiev, E. G. Gamaly, O. N. Krokhin, and V. B. Rozanov, Sov. Phys. JETP **44**, 311 (1976).